Self-Reversal Phenomena of Toroidal Current by Reversing the External Toroidal Field in Helicity-Driven Toroidal Plasmas

M. Nagata,[1] T. Oguro,[1] Y. Kagei,[1] K. Kawami,[1] H. Hasegawa,[1] N. Fukumoto,[1] M. Iida,[2] S. Masamune,[2] M. Katsurai,[3] and T. Uyama[1]

[1]*Department of Electrical Engineering and Computer Sciences, Himeji Institute of Technology, Hyogo 671-2201, Japan*
[2]*Department of Electronics and Information Science, Kyoto Institute of Technology, Kyoto 606-8585, Japan*
[3]*Department of Advanced Energy, University of Tokyo, Tokyo 113-8656, Japan*

(Received 6 January 2003; published 6 June 2003)

In order to understand self-organization in helicity-driven systems, we have investigated the dynamics of low-aspect-ratio toroidal plasmas by decreasing the external toroidal field and reversing its sign in time. Consequently, we have discovered that the helicity-driven toroidal plasma relaxes towards the flipped state. Surprisingly, it has been observed that not only toroidal flux but also poloidal flux reverses sign spontaneously during the relaxation process. The self-reversal of the magnetic fields is attributed to the nonlinear growth of the $n = 1$ kink instability of the central open flux.

DOI: 10.1103/PhysRevLett.90.225001 PACS numbers: 52.55.Wq, 52.30.Cv

Steady-state magnetic helicity injection using coaxial electrodes has successfully demonstrated noninductive current generation in spheromaks and low-aspect-ratio torus/tokamaks (spherical torus: ST) that have a potential to lead to an attractive high-beta fusion reactor on CTX, SPHEX, FACT/HIST, SSPX, HIT-II, and NSTX [1–7]. Magnetic field fluctuations with toroidal mode number $n = 1$ excited by coaxial helicity injection (CHI) have been observed in all those machines. This fact implies that nonaxisymmetric dynamic processes create the dynamo action in the plasmas and relaxes them toward certain minimum energy equilibria: The helicity injection is based on both Cowling's theorem [8] and the Taylor driven-relaxation principle [9,10]. The $n = 1$ fluctuations, which arise from a current-driven helical kink instability on the open flux, could be responsible for the formation and sustainment of the configurations by helicity injection [11]. The main purpose of this work is to reveal the essential role of the $n = 1$ relaxation activity in self-organization, current generation, and transitions between various helicity-driven relaxed states of low-aspect-ratio toroidal plasmas: STs, spheromaks, and spherical reversed-field pinches (RFPs). Helicity is defined as linked magnetic fluxes; the experiment is a demonstration of its approximate conservation even in a strongly perturbed system.

In the HIST device at Himeji Institute of Technology [4], we have investigated the time evolution of ST plasmas by decreasing the strength of the external toroidal field (TF) and reversing rapidly the direction of the TF-coil current I_{tf} during the helicity injection phase. This is a useful way to create the $n = 1$ resonant surface in a tokamak although it is not normally carried out, since ST plasmas, which are usually operated with the safety factor $q > 1$, must pass through the major rational ratio of $m = 1/n = 1$, i.e., violation of the Kruskal-Shafranov stability condition [12]. It is widely known that, by reversing I_{tf} quickly during the early stage of the current ramp-up phase, an RFP configuration is produced without a major disruption, through a spontaneous dynamo related to the excitation of resistive tearing modes. One would expect the formation of the RFP configuration in the driven system as well, but it is not maintained by flux conversion because there is no poloidal current externally driven by an Ohmic transformer. Here, a fundamental question is how the helicity-driven ST plasma evolves nonlinearly after passing through the $q = 1$ rational barrier.

In this Letter, a most attractive finding is that the ST plasmas do not collapse after passing through the $q = 1$ rational barrier, but relax towards a novel relaxed configuration, that is, the flipped ST which has not previously been found experimentally. The structural formation of the flipped field configuration incorporates the self-reversal process of the toroidal and poloidal (toroidal plasma current) fields. We have examined the self-reversal process and the transition between relaxed states by measuring temporal evolutions of internal magnetic field and current structures. This self-organizing phenomenon may have some analogy to reversal of the dipole field of Earth generated by a dynamo action [13]. It is fundamentally important to elucidate a current-reversal phenomenon occurring in space and laboratory plasmas.

The driven-relaxed configurations with open field lines, as well as closed systems, are described by the force-free equilibrium equation, $\nabla \times \mathbf{B} = \lambda \mathbf{B}$, where the force-free parameter $\lambda = \mu_0 \mathbf{J} \cdot \mathbf{B}/B^2 = \text{const}$ [10]. The nature of these relaxed states in toroidal systems is characterized by the strength of the external toroidal field and the value of λ determined by coupling to a helicity source. The constant-λ value is ideally controlled by the gun source parameter $\lambda_g = \mu_0 I_{\text{gun}}/\Psi_{\text{bias}}$, where I_{gun} is the gun current and Ψ_{bias} is the bias flux. The equilibrium analysis presented in Ref. [14] on the basis

of the helicity-driven relaxation theory [10] predicts that a flipped ST plasma is formed when the external toroidal flux $\Psi_{t.e}$ is negative ($\Psi_{t.e} < 0$).

By using the analytical solution of the force-free equation in a rectangular flux conserver (FC) that was presented in Ref. [15], we have calculated relaxed configurations with"open" magnetic field lines penetrating the boundaries in both cases $\Psi_{t.e} > 0$ and $\Psi_{t.e} < 0$. The toroidal field B_t is expressed as $\lambda\Psi/r$, where Ψ is the flux function and r is the radius. The strength of vacuum toroidal field $B_{t.e}$ is given by a value of $\Psi = \mu_0 I_{tf}/2\pi\lambda$ at the FC wall boundary. Figure 1 shows the amount of poloidal flux Ψ_p as a function of $\Psi_{t.e}$ normalized by Ψ_{bias} and poloidal flux contours for each region: ST, RFP, flipped ST, and flipped RFP. For fixed $\lambda = 8.44$ close to the lowest eigenvalue $\lambda_e = 8.53$, as $\Psi_{t.e}$ varies continuously from a positive to a negative value, we can see that, at a certain value of $\Psi_{t.e} < 0$, the normal ST 1(A) gets to RFP-like state 1(B), then as $\Psi_{t.e}$ is reduced further, a small island of reversed poloidal flux 1(C) appears from the right side, leading to the flipped states 1(D). There are clear differences in magnetic topology between "normal" ST and "flipped" ST. It should be noted that the open flux no longer surrounds the closed flux in the flipped state since the toroidal current is in the opposite direction (the bias poloidal flux has the same direction), but directly joins the gun electrodes by the shortest path. For a ST with a lower λ (higher q), the ratio of the closed poloidal flux to the total flux becomes smaller. Note that the ST must cross the RFP region transiently for the transition to the flipped ST. As for $\lambda > \lambda_e$, there are flipped RFP states ($\Psi_{t.e} > 0$) 1(E) and normal RFP states with a significant amount of closed flux ($\Psi_{t.e} < 0$) 1(F). As for the spheromak without a central conductor, when λ becomes slightly above λ_e, it is flipped [16]. Note that in the doubly connected toroidal system, on the other hand, the flipped ST state appears in the regime of $\lambda < \lambda_e$, so that it could be observed in experiments.

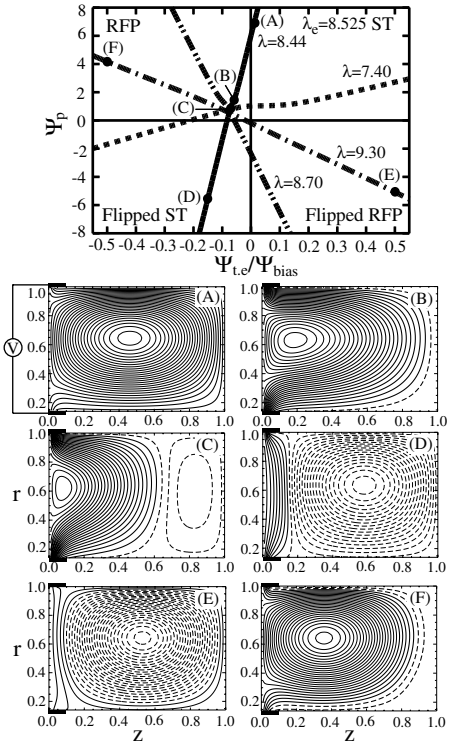

FIG. 1. Poloidal flux as a function of $\Psi_{t.e}/\Psi_{bias}$ for $\lambda = 7.40$, 8.44, 8.60, and 9.30 m^{-1}, where $\lambda_e = 8.53$ m^{-1}. Contour plot (A) shows ST with open flux going around the outside of the closed flux. (B) shows RFP-like configurations with open reversed flux. We see in (C) that the closed (reversed) flux comes out from the right side of FC. (D) represents flipped ST with closed (reversed) flux which is isolated from electrodes. (E) and (F) show Flipped RFP and RFP, respectively. Dashed lines in all contour plots denote the reversed magnetic flux.

The HIST device and diagnostics, shown in Fig. 2, has a major radius $R = 0.30$ m, minor radius $a = 0.24$ m, aspect ratio $A = 1.25$, toroidal field $B_t < 0.2$ T, peak plasma current $I_t < 150$ kA, and discharge time $t < 5$ ms for the ST configuration [4]. The magnetized coaxial plasma gun (MCPG) is operated with formation capacitor banks (13 kJ, 5 kV) and sustainment banks (61 kJ, 600 V). The I_{gun} and gun voltage V_{gun} are ≈ 25 kA, and ≤ 0.5 kV, respectively, and the bias flux Ψ_{bias} produced around the MCPG muzzle is 0.8–1.1 mWb in this experiment. The TF-coil current I_{tf} is varied from +20 kA to $0 \sim -60$ kA. A three axis magnetic probe (nine channels each for B_r, B_ϕ, B_z) is located in the plasma at a distance of $z = -0.75$ m from the midplane ($z = 0$ m) of the flux conserver. Magnetic pickup coils (26 channels each for B_p, B_t) are located in the poloidal direction along the inner surface of the spherical solid copper FC (diameter: 1.0 m; thickness: 3 mm) to calculate the total toroidal current I_t. A six channel λ probe incorporating small size Rogowski and flux loops is used to measure toroidal current density and toroidal flux profiles on the FC midplane. The toroidal n mode number of the magnetic fluctuations of B_t is measured using eight magnetic

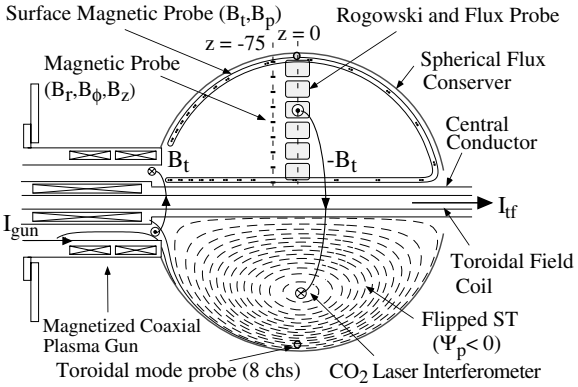

FIG. 2. The schematic drawing of the HIST device and diagnostics.

pickup coils distributed toroidally at equal angles over 360° around the outer edge. The line averaged electron density measured by a CO_2 laser interferometer is in the range of (1–5) $\times 10^{19}$ m^{-3}. The electron temperature is in the range 20–40 eV. The vacuum base pressure reaches 2×10^{-9} Torr after titanium coating on the FC.

Figure 3 shows the time evolution of I_t for three different values of the reversed I_{tf} (− 20, −27, and −50 kA at the peak time). The ST plasmas with a peak toroidal current I_t of 80 kA are initially produced by CHI and the reversed-TF circuit is triggered at $t = 0.16$ ms during the current ramp-down phase. The time scale over which I_{tf} changes is quite slow (≈ 0.5 ms) compared with an Alfvén time. When I_{tf} is reduced to −20 kA, the toroidal current I_t and the averaged paramagnetic toroidal field $\langle B_{t.c} \rangle$ in the central core region reverse. For increasingly negative values of I_{tf}, the reversal time of I_t tends to shift to earlier times. The critical value of the TF-coil current required for the current reversal is $I_{tf} \approx -20$ kA. In these discharges, the I_t of flipped plasmas decays smoothly due to its resistivity.

Reversing the TF-coil current during the early stage of the current ramp-up phase, we found that the RFP-like profile is transiently created during the discharge as expected. Figure 4 shows the time evolution of I_t and radial profiles of poloidal magnetic field (axial component B_z and radial component B_r), toroidal magnetic field B_t, and vacuum toroidal field (dotted line) at each time [4(a)–4(d)]. An initial plasma is produced by CHI which presents a ST-like configuration [Fig. 4(a)]. After turning on the reversed-TF circuit at $t = 0.36$ ms in the ramp-up phase, the paramagnetic toroidal field $\langle B_{t.c} \rangle$ in the core region significantly amplifies due to rapid inward diffusion of poloidal current inductively generated at edges. Subsequently, the toroidal field at the edge regions decreases rapidly and reverses the sign slightly, which results in the formation of an "axisymmetric" RFP-like configuration [Fig. 4(b)]. This configuration does not remain for a long time, and then quickly enters into the relaxation phase ($t = 0.6$–0.69 ms) in which a large distortion of the magnetic profiles is seen at $t = 0.63$ ms [Fig. 4(c)]. After both the poloidal and toroidal fields reverse sign spontaneously during the relaxation, the axisymmetric magnetic field configuration of the flipped ST is formed at $t = 0.74$ ms [Fig. 4(d)]. The continuity of the averaged electron density is seen throughout the discharge.

In order to investigate the generation process of the RFP-like configuration and the subsequent current-reversal process, we have measured the time evolution of modes with toroidal mode number n and the toroidal current density profile $J_t(R)$. The λ value is estimated by $\lambda_{co} \equiv \mu_0 I_t / \Psi_t$ averaged in the central core region ($R = 0.21$–0.34 m) and the q_0 value around the magnetic axis is approximately given by the formula of $q_0 \equiv 2/R\lambda_{co}$ [14], where R is the major radius. We note that the meanings of λ_{co} and q_0 are not well defined during the relaxation. The initial ST has a value $\lambda_{co} \approx 3$ m^{-1} ($q_0 \approx 2$). Figure 5 shows that the previously hollow current profile becomes peaked around the magnetic axis ($R = 0.32$ m) for $t = 0.52$–0.54 ms due to anomalous inward current penetration so that λ_{co} continues to increase until it is just below the critical value of λ_e ($= 9.3$ m^{-1}). The RFP-like configuration with $q_0 \approx 0.67$ is formed during the quiescent period of $t = 0.54$–0.56 ms, where the amplitude of $n = 1, 2, 3$ modes is relatively very low. After this stable phase, the growth of the $n = 1$ mode causes the current profile to deform

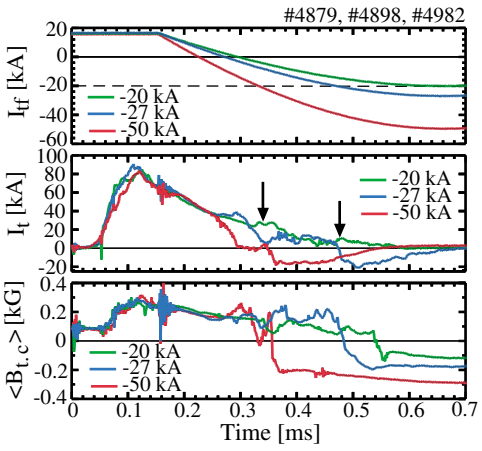

FIG. 3 (color). The time-dependent data from discharges in reversing the TF coil current I_{tf}. I_t is the toroidal current and $\langle B_{t.c} \rangle$ is the toroidal field averaged in the core region.

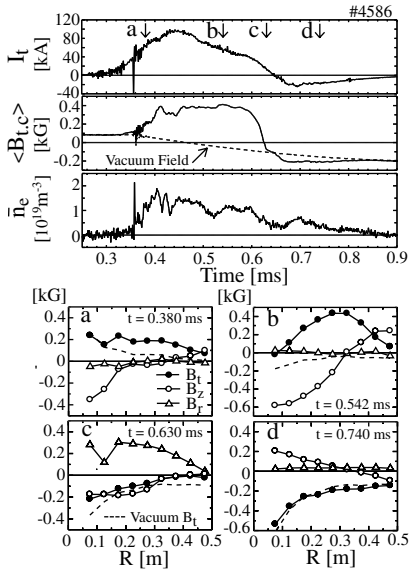

FIG. 4. Typical discharge showing the transition from ST through RFP to flipped ST. Radial profiles of poloidal field B_p, toroidal field B_t, and vacuum toroidal field of ST (a), RFP (b), and flipped ST (d) formed in a decaying mode. $\bar{n}_e$ is the line-averaged electron density.

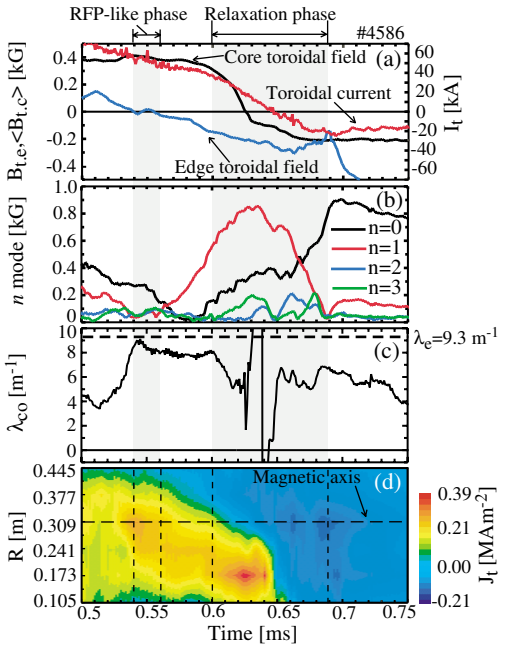

FIG. 5 (color). Time evolutions of I_t, $\langle B_{t,c}\rangle$, $B_{t,e}$ (a), amplitude of n modes (b), λ_{co} (c), and contour plots of toroidal current density profile J_t (d), during the self-organization phase.

highly and the outer reversal point of $J_t(R)$ begins to shift towards the central conductor. Consequently, the toroidal current appears to concentrate on the inner edge region ($R = 0.17$ m) and to stay there during $t = 0.61$–0.64 ms. This behavior suggests the nonlinear saturation of the $n = 1$ kink mode of the central open column. At the same period, the $n = 2, 3$ modes are being excited owing to nonlinear coupling. Afterwards, the remaining part of positive toroidal current changes the sign abruptly at $t = 0.65$ ms and the toroidal current profile is redistributed by the relaxation. After a sufficient damping of the amplitude of the $n = 1$ mode, the axisymmetric flipped configuration is established. Here, it is likely that the safety factor q_0 of the flipped ST is bounded above $q_0 = 1$ (corresponding to $<\lambda_{co} = 6.5\ \mathrm{m}^{-1}$) by the Kruskal-Shafranov criterion.

Three-dimensional MHD numerical simulations [17] have succeeded in demonstrating the formation of the flipped ST and substantially enabled us to understand the nonlinear dynamic field-reversal mechanisms. The simulation results indicate that a large helical distortion of the open flux and the following magnetic reconnection between open and closed field lines play a major role in the self-reversal process. The manner of growth of toroidal n modes in the simulation agrees well with experiment. A stability analysis [18] indicated that the configuration including open flux linked to the electrodes becomes linearly unstable to an ideal MHD kink instability, if λ in the open flux region is sufficiently large. During the transition, an unstable plasma with high λ in the open flux region relaxes to a stable one with low λ. These results are in good agreement with the present experimental observations.

In conclusion, the most important discovery of this experiment is that ST plasmas tend to self-organize to the flipped states while reversing the direction of TF. This experimental finding provides, for the first time, evidence for the existence of the relaxed states which were theoretically predicted. The observation of the self-reversal phenomena suggests strongly that the sign of helicity $K = c\Psi_p\Psi_t$ $(1 < c < 2)$ for any toroidal plasma, where c depends on the plasma shape and current profile, is conserved with significant losses in the magnitude during the relaxation, namely, when Ψ_t in the flipped plasma region becomes negative, then Ψ_p must also be so. The linkage of the gun magnetic flux with the rest of the plasma may not be conserved in the transition from regular to flipped topologies. A quantitative proof of the helicity conservation is an important work in our future experiments and numerical simulations. The elementary reversal mechanism is closely related to the magnetic reconnection of the helically kinked open field lines surrounding the closed flux surfaces. From the viewpoint of helicity injection current drive, it is conceivable that the flipped ST compares favorably with the normal ST, because it consists of only closed flux surfaces.

The authors are grateful to P. K. Browning for valuable discussions and suggestions.

[1] T. R. Jarboe *et al.*, Phys. Rev. Lett. **51**, 39 (1983).
[2] P. K. Browning *et al.*, Phys. Rev. Lett. **68**, 1722 (1992).
[3] M. Nagata *et al.*, Phys. Rev. Lett. **71**, 4342 (1993).
[4] M. Nagata *et al.*, in *Fusion Energy 1998* (IAEA,Vienna, 2000), CD-ROM file, EXP4/10.
[5] H. S. McLean *et al.*, Phys. Rev. Lett. **88**, 125004 (2002).
[6] T. R. Jarboe *et al.*, Nucl. Fusion **41**, 679 (2001).
[7] R. Raman *et al.*, Nucl. Fusion **41**, 1081 (2000).
[8] T. G. Cowling, Mon. Not. R. Astron. Soc. **94**, 39 (1934).
[9] J. B. Taylor, Phys. Rev. Lett. **33**, 1139 (1974).
[10] J. B. Taylor and M. F. Turner, Nucl. Fusion **29**, 219 (1989).
[11] S. Woodruff and M. Nagata, Plasma Phys. Controlled Fusion **44**, 2539 (2002).
[12] G. Bateman, *MHD Instabilities* (MIT Press, Massachusetts, 1980), p. 107.
[13] J. Li, T. Sato, and A. Kageyama, Science **295**, 1887 (2002).
[14] P. K. Browning *et al.*, Plasma Phys. Controlled Fusion **35**, 1563 (1993).
[15] R. Ono and M. Katsurai, IEE (Japan) **117-A**, 591 (1997).
[16] P. M. Bellan, *Spheromaks* (Imperical College Press, London, 2000), Chap. 11.
[17] Y. Kagei *et al.*, Plasma Phys. Controlled Fusion **45**, L17 (2003).
[18] D. P. Brennan, P. K. Browning, and R. A. M. Van der Linden, Phys. Plasmas **9**, 3526 (2002).